

Tunable work function in MgO/Nb:SrTiO₃ surfaces studied by Kelvin probe techniqueTomofumi Susaki,^{*} Asahi Makishima, and Hideo Hosono[†]*Secure Materials Center, Materials and Structures Laboratory, Tokyo Institute of Technology, Nagatsuta, Midori, Yokohama 226-8503, Japan*

(Received 24 November 2010; revised manuscript received 24 January 2011; published 16 March 2011)

We studied the work function of Nb 0.5-wt % doped SrTiO₃ (Nb:SrTiO₃) (100) substrates covered with MgO thin films by Kelvin probe contact potential technique. The work function of MgO/Nb:SrTiO₃ was reduced as a sharp function of MgO film thickness up to 1 nm while it remained almost constant beyond 1 nm. The amount of work-function reduction by depositing 5-nm-thick MgO film was ~ 0.6 eV when grown under oxygen partial pressure, $p(\text{O}_2)$, of 10^{+1} Pa and increased up to ~ 1 eV when grown at $p(\text{O}_2) = 10^{-3}$ Pa. Atomic force microscopy and in-plane x-ray-diffraction measurements indicated the formation of tighter interface when grown under oxygen poor conditions. Both a sharp work-function reduction with MgO deposition and its modification by how firmly the interface was formed were consistent with the electron compression model that the metal work function could be modified when covered by insulating films to block the metal electrons. The present work demonstrated that metal work function could be tuned by depositing insulating films with the film thickness and the interfacial tightness controlled.

DOI: 10.1103/PhysRevB.83.115435

PACS number(s): 73.30.+y, 73.40.Ns

I. INTRODUCTION

Artificial structures have opened possibilities to study novel electronic states as well as to develop various electronic and catalytic functionalities. Among various artificial structures, the most fundamental is a single interface between metal and insulator, where two materials with opposite electrical characters are contacted to each other, inducing significant changes in the electronic states of both sides.¹ Recently, a large change in metal work function by depositing thin insulating films has been attracting much attention since work function is a fundamental physical quantity in surface and interface physics and is crucial to develop any functionalities in electronics and in catalysis. Density-functional calculations have revealed that metal work function can decrease by a few eV as insulating films are deposited.²⁻⁵ A dominant origin of such a decrease is the compression of metal electrons by the insulating layer: Usually dipole moments are present at the surface of metal since electrons are slightly spilling out from the lattice of positive ions. Capping with an insulating layer pushes back the leaking electrons, varying the surface dipole moments and hence the metal work function. Such effect strongly depends on the interface separation, i.e., how tightly or loosely the interface is formed.^{2,5} An ideal hard wall potential at the tightly formed interface would significantly modify the surface electronic states while a loosely formed interface should be similar to a free surface. The effect of electron compression is particularly dominant for wide gap insulators while the effect of charge transfer between metal and insulator increases as the band gap decreases.

In order to demonstrate the electron compression effect, MgO(100) thin film can be a model system since high quality MgO(100) thin film keeps the wide gap electronic structure characteristic of bulk MgO even at the very interface.⁶ Very recently, the work function of MgO thin films deposited on elemental metals has been measured by Kelvin probe force microscopy,^{7,8} by scanning tunneling microscopy,⁷ and by photoemission spectroscopy,⁹ where a sharp drop of metal work function by depositing MgO thin film has indeed been revealed.

In the present work we have measured the work function of Nb 0.5-wt % doped SrTiO₃ (Nb:SrTiO₃) (100) substrates covered with MgO thin films by *macroscopic* Kelvin probe contact potential technique. Since Nb:SrTiO₃(100) is a representative conducting substrate for oxide thin-film growth and MgO/metal interfaces play key roles in various electronic devices including Fe/MgO/Fe magnetic tunneling junctions,¹⁰ the tunable work function in MgO/Nb:SrTiO₃(100) would be valuable to develop any oxide electronic devices. Considering a finite electrode size in electronic devices, which is much larger than the probe size of Kelvin force microscopy (15–30 nm radius⁷), *macroscopic* work-function measurement should be relevant for this purpose. Also, compared with microscopic Kelvin probe, the parallel-plate capacitor geometry, which gives a homogeneous electric field, and the large gap between probe and sample would allow a simpler interpretation in macroscopic Kelvin probe. We have found that the work function of Nb:SrTiO₃(100) is indeed strongly reduced by depositing a very thin MgO film and that the oxygen partial pressure during growth, $p(\text{O}_2)$, can be another parameter governing the “interface tightness” to control the work-function reduction. Such MgO film thickness dependence and $p(\text{O}_2)$ dependence of work function in MgO/Nb:SrTiO₃(100) have consistently been understood in the framework of the electron compression model. The present surface with tunable work function made of a representative wide gap insulator and a representative conductive substrate would be useful as a platform to develop various electronic and catalytic functionalities.

II. EXPERIMENT

We grew MgO thin films on Nb:SrTiO₃(100) substrates by pulsed laser deposition. A MgO single-crystal target was irradiated by a KrF excimer laser with the repetition ratio of 1 Hz and with the energy of ~ 100 mJ incident to the vacuum chamber. The deposition rate was between 0.8 and 0.12 nm/min. A cycle of MgO thin-film growth and work-function measurement was performed without exposing the sample

surface to air. The substrate mount was set at $\sim 740^\circ\text{C}$ for 20 min before film growth and was kept at the same temperature during film growth. Samples were transferred to a stable platform for the Kelvin probe measurement after being cooled down to $\sim 200^\circ\text{C}$.

We used a 4-mm ϕ stainless-steel plate as a counterelectrode for Kelvin probe measurement (KP Technology). We applied an external offset voltage between the counterelectrode and the backside of Nb:SrTiO₃ substrate. When the counterelectrode is brought close to a sample surface, charges are induced both at the counterelectrode and at the sample surface in accord to the electric field originating from the difference of the vacuum level between them. Since such an electric field depends on the distance between the counterelectrode and sample, vibration of the counterelectrode induces an alternating current corresponding to the oscillating charge at the counterelectrode. By applying an offset voltage to the counterelectrode so that the vacuum level is aligned between the electrode and sample surface, the alternating current should be reduced to zero. By this way the work function of sample surface can be measured with respect to the counterelectrode. Finally we calibrated the work function of stainless counterelectrode by defining the observed work function of *in situ* deposited gold to be 5.1 V.¹¹

We set $p(\text{O}_2)$ between 10^{+1} and 10^{-3} Pa during the film growth and kept the same pressure during the work-function measurement. After ~ 10 cycles of film growth and work-function measurement, the total MgO film thickness (about 5 nm) was measured by x-ray reflection measurements. The samples were further characterized by atomic force microscopy (AFM) and by x-ray diffraction (XRD). The data of Fig. 1 (out-of-plane XRD), Fig. 2 (AFM), Fig. 3 (in-plane XRD), and Fig. 4 (Kelvin probe measurements) were taken for the same set of five samples, which were grown at $p(\text{O}_2) = 10^{+1}$ – 10^{-3} Pa.

III. RESULTS

Figure 1 shows out-of-plane XRD patterns of MgO films with the thickness of ~ 5 nm grown on Nb:SrTiO₃(100), indicating the (100) oriented growth of MgO films. No systematic change was observed as a function of $p(\text{O}_2)$ from 10^{+1} to 10^{-3} Pa. Small peaks at $\sim 38^\circ$, $\sim 64^\circ$, and $\sim 77^\circ$, which are missing in the pattern of a bare Nb:SrTiO₃ substrate, would not be assigned to other diffractions of MgO and their origins are not clear: These positions are different by more than $\sim 1^\circ$ from expected MgO 111, 220, and 222 diffraction angles. Also, the two angles of $\sim 38^\circ$ and $\sim 77^\circ$ are not consistently interpreted with a single d_{111} value.

Figures 2(a)–2(e) show 5×5 - μm AFM scans of MgO films grown at various $p(\text{O}_2)$ on Nb:SrTiO₃(100) substrates. No clear structure or pattern is present in the surface of samples. The root-mean-square (rms) surface roughness estimated by these scans is shown in Fig. 2(f) as a function of $p(\text{O}_2)$. It is as small as ~ 2 Å between 10^0 and 10^{-3} Pa but increases up to ~ 5 Å at 10^{+1} Pa.

In Fig. 3(a) we plot in-plane XRD patterns of ~ 5 -nm-thick MgO films grown on Nb:SrTiO₃(100) substrates and show the lattice constant deduced from the MgO 010 peak position in Fig. 3(b). Although the bulk lattice constant of SrTiO₃ is $\sim 8\%$ smaller than that of MgO, the observed in-plane lattice

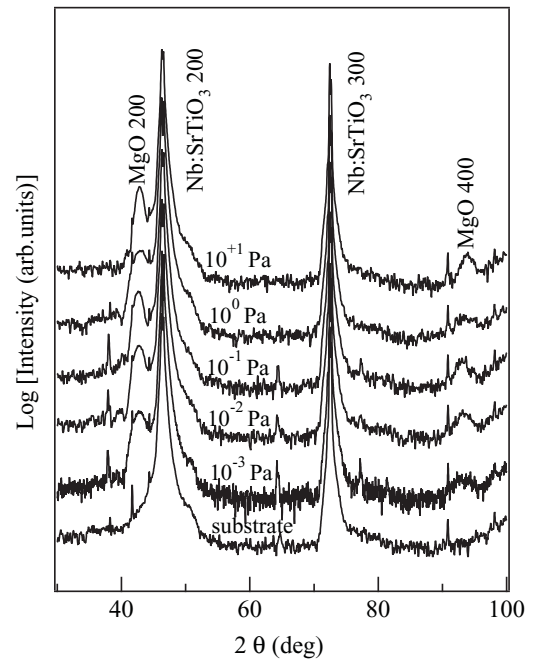


FIG. 1. Out-of-plane XRD patterns of MgO films with the thickness of ~ 5 nm grown on Nb:SrTiO₃(100) substrates at $p(\text{O}_2) = 10^{+1}$ – 10^{-3} Pa. XRD pattern of Nb:SrTiO₃(100) substrate is also shown.

constant of MgO films is $\sim 1\%$ smaller than the bulk value when grown between $p(\text{O}_2) = 10^0$ and 10^{-3} Pa and is only $\sim 0.3\%$ smaller at $p(\text{O}_2) = 10^{+1}$ Pa. This shows that ~ 5 -nm-thick MgO films thus grown on Nb:SrTiO₃(100) is only partly strained when grown under oxygen poor conditions and is almost completely relaxed otherwise. The cubic on cubic in-plane relationship between MgO and Nb:SrTiO₃ with the film lattice constant almost relaxed has also been observed in MgO films on nondoped SrTiO₃(100) substrates grown by plasma assisted molecular-beam epitaxy.¹²

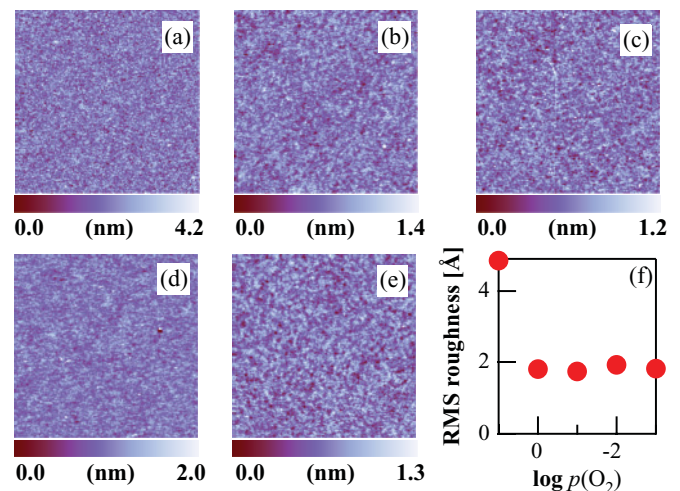


FIG. 2. (Color online) 5×5 - μm AFM scan of MgO/Nb:SrTiO₃(100) grown at $p(\text{O}_2) = 10^{+1}$ Pa (a), 10^0 Pa (b), 10^{-1} Pa (c), 10^{-2} Pa (d), and 10^{-3} Pa (e). A root-mean-square surface roughness estimated from scans (a)–(e) is shown in panel (f).

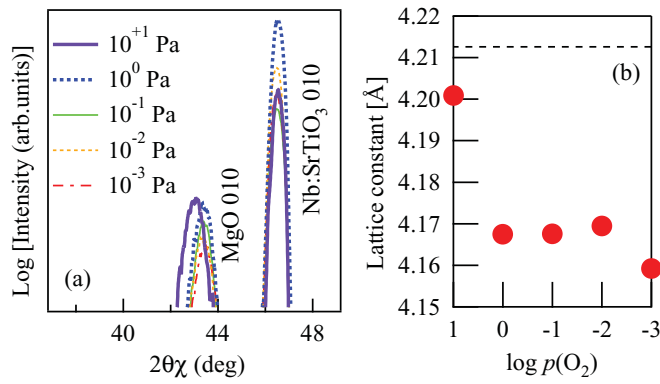


FIG. 3. (Color online) (a) In-plane XRD patterns of MgO/Nb:SrTiO₃(100) parallel to Nb:SrTiO₃[010] direction. Bold curve, bold dots, thin curve, thin dots, and thin dot-dashed curve correspond to XRD patterns of MgO films grown at $p(\text{O}_2) = 10^{+1}, 10^0, 10^{-1}, 10^{-2},$ and 10^{-3} Pa, respectively. (b) In-plane lattice constants of MgO/Nb:SrTiO₃(100) estimated from the MgO 010 peak position in (a). The bulk lattice constant of MgO is shown by a dashed line.

The work function of MgO/Nb:SrTiO₃(100) grown at various $p(\text{O}_2)$ has been measured by Kelvin probe contact potential technique as shown in Fig. 4. The values of the work function for bare Nb:SrTiO₃(100) substrates is distributed at 4.8–4.4 eV, which is slightly larger than a reported value of nondoped SrTiO₃ (4.2 eV).¹³ As MgO film thickness increases up to ~1 nm, the work function is significantly reduced. The thickness dependence of the work function is small beyond the film thickness of 1 nm. Here, a change in the work function with MgO film thickness is larger when grown under oxygen poor conditions. We have grown several samples with ~5 nm thickness under each growth condition and the reproducibility is as shown in Fig. 5, indicating that the work function of MgO/Nb:SrTiO₃(100) linearly changes as a function of $\log p(\text{O}_2)$ while that of Nb:SrTiO₃(100) substrates depends very weakly on $p(\text{O}_2)$ during preannealing (~0.2 eV decrease in going from 10^{+1} to 10^{-3} Pa). The work-function reduction by depositing 5-nm-thick MgO is ~0.6 eV at $p(\text{O}_2) = 10^{+1}$ Pa and is ~1 eV at $p(\text{O}_2) = 10^{-3}$ Pa.

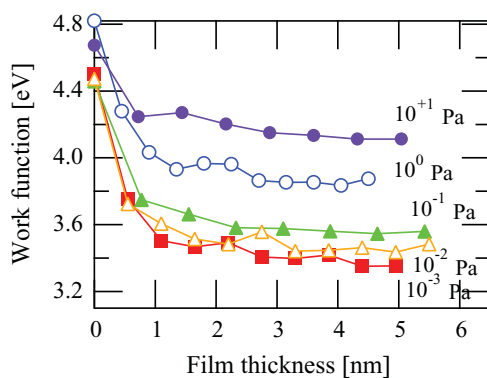


FIG. 4. (Color online) Work function of MgO/Nb:SrTiO₃(100) as a function of MgO film thickness: closed circles (10^{+1} Pa), open circles (10^0 Pa), closed triangles (10^{-1} Pa), open triangles (10^{-2} Pa), and squares (10^{-3} Pa).

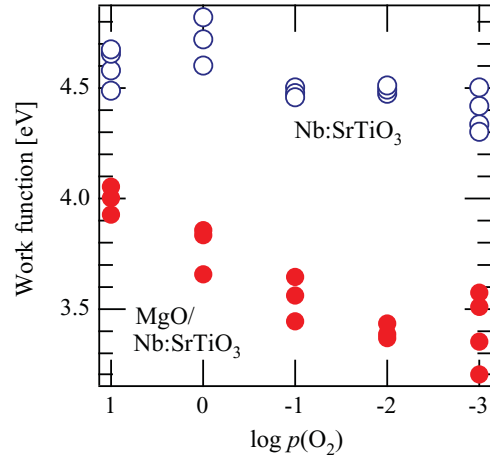


FIG. 5. (Color online) Work function of ~5-nm-thick MgO grown on Nb:SrTiO₃(100) (closed circles) and bare Nb:SrTiO₃(100) substrates (open circles) as a function of $p(\text{O}_2)$.

IV. DISCUSSION

In general, the interpretation of Kelvin probe measurement of insulating films is not straightforward.^{14,15} However, MgO films in the samples studied here are grown along the nonpolar [001] direction and are as thin as 5 nm, which is much smaller than the distance between sample and reference electrode (0.1–0.5 mm). Then charge oscillation in the reference electrode should reflect the charge oscillation in Nb:SrTiO₃(100) substrate, where the work function can be modified from the bulk value. This picture should be relevant when MgO film is perfectly insulating and is very thin: When no electronic states are present around the Fermi level in the MgO layer, no electrons can emit from that layer even if an energy corresponding to the work function of MgO film is externally given. Instead, electrons excited above the vacuum level in Nb:SrTiO₃ should be ejected into the vacuum: When the vacuum level is lower in the MgO layer than that in the Nb:SrTiO₃ substrate, the MgO layer does not affect “free electrons” from Nb:SrTiO₃. Even when the vacuum level is higher in the MgO layer, free electrons would tunnel through that.

According to this interpretation, a sharp drop of the work function of Nb:SrTiO₃(100) surface by depositing a small amount of MgO is consistent with the electron compression effect induced by the hard wall type potential of MgO, which has been revealed in recent theoretical^{2–5} and experimental^{7–9} studies on elemental metal substrates. A small difference from reported behaviors is observed in thickness dependence: While the work function of MgO/Nb:SrTiO₃(100) strongly depends on the film thickness up to 1 nm, the work function does not change at all beyond two to three monolayers (0.4–0.6 nm) in MgO/Ag(100) and MgO/Mo(100). Since both MgO and Nb:SrTiO₃ are metal oxides and share a framework of electronic structure with the oxygen derived valence band and cation derived conduction band, a larger electronic mixing would be present in the MgO/Nb:SrTiO₃ interface, resulting in a deviation from the “hard wall” picture of MgO. Such a deviation might be one of the origins of the work-function change observed in larger thickness regions in MgO/Nb:SrTiO₃(100).

The effect of smaller carrier concentration in Nb:SrTiO₃ than in elemental metals should also be clarified in the future.

The effect of $p(\text{O}_2)$ is clear and systematic as shown in Fig. 5. According to Fig. 3, the lattice constant of MgO films is more influenced by the substrate when grown under oxygen poor conditions. Together with formation of a flat surface in MgO films grown under oxygen poor conditions according to AFM measurements (Fig. 2), a tighter interface would be formed when grown under oxygen poor conditions. Thus the present oxygen pressure dependence would reflect that the formation of abrupt hard wall potential at the very surface of metallic substrate gives a stronger reduction of work function according to the electron compression model as predicted in density-functional calculations.^{2,4,5}

Here, oxygen vacancies in MgO films, which could depend on $p(\text{O}_2)$ and could be charged, would possibly contribute to the pressure dependent work function. However, since the MgO films grown on insulating Al₂O₃(0001) substrates under the same condition have been found insulating and since the formation of oxygen vacancies has been reported to induce the lattice expansion in MgO,¹⁶ which is the tendency opposite to the present lattice constant change, the effect of oxygen vacancy formation would be small in the present case. The observation that the work function strongly varies only below the film thickness of 1 nm also suggests that a uniform formation of charged vacancies in MgO films during the film growth is unlikely. Nevertheless, a possibility of oxygen vacancy formation at the very interface would not be excluded: Density-functional calculations have shown that oxygen vacancy formation is not unfavorable in MgO substrate in SrTiO₃/MgO(100) interface although they consider a SrTiO₃ film on a MgO substrate, opposite to the interface studied here.¹⁷ Also, while the work function shows a quite smooth variation with $p(\text{O}_2)$ as shown in Fig. 5, the structural parameters show a significant difference between $p(\text{O}_2) = 10^1$ and 10^0 Pa, as shown in Fig. 2(f) and in Fig. 3(b), implying that the interfacial tightness is not the unique parameter which is controlled by $p(\text{O}_2)$. A direct observation of chemical stoichiometry and abruptness at the very interface as well as the interface separation would be critical to elucidate the role of oxygen partial pressure during film growth.

Another possible origin of pressure dependent work function would be incomplete capping under oxygen rich conditions, giving a surviving contribution of Nb:SrTiO₃ substrates. Then the work function of MgO/Nb:SrTiO₃ grown under various conditions should converge on a single value as the nominal film thickness increases. However, Fig. 4 shows that

the $p(\text{O}_2)$ dependence at 5 nm is as large as at 1 nm, indicating that such incomplete capping effect is small.

V. CONCLUSION

We have measured *in situ* the work function of MgO/Nb:SrTiO₃(100) with the film thickness up to 5 nm by Kelvin probe contact potential technique and have found that the work function of MgO/Nb:SrTiO₃ can be controlled both by MgO film thickness and by $p(\text{O}_2)$, i.e., a tunable work function has been realized by using a representative wide gap insulator and a representative oxide substrate.

A change in the work function is almost completed at the MgO film thickness of 1 nm, qualitatively consistent with the electron compression model that the hard wall type potential of insulating film blocks the leaking metal electrons to modify the metal work function. The reduction of work function increases when MgO films are grown under oxygen poor conditions: For 5-nm-thick MgO films it is ~ 0.6 eV at $p(\text{O}_2) = 10^{+1}$ Pa and amounts to ~ 1 eV at $p(\text{O}_2) = 10^{-3}$ Pa. Together with $p(\text{O}_2)$ dependence of in-plane x-ray-diffraction and AFM measurements, the $p(\text{O}_2)$ dependence of the work function would indicate that the work function of MgO/Nb:SrTiO₃ can be controlled also by $p(\text{O}_2)$ through the interface separation change, again consistent with the electron compression model.

While we have focused on perfectly insulating and very thin MgO films in the present work, thick MgO films with possible impurities would also be of great interest: A smaller work function realized in MgO would induce a high secondary electron emission yield,¹⁸ which is relevant for the protective layer of dielectric layers in plasma display panels.¹⁹ Remembering that MgO shows various catalytic activities including hydrogen extraction from methane,^{20,21} dissociation of water,²² and reduction of CO₂ to CO,²³ and that the correlation between catalytic activities and the work function in MgO thin films on metal substrates have intensively been studied,^{24,25} to study catalytic properties in MgO/Nb:SrTiO₃ with the controlled work function would be another straightforward program based on the present work.

ACKNOWLEDGMENTS

We thank Toshio Kamiya for critical discussions and Yoshitaka Honda, Kosuke Matsuzaki, Kyeongmi Lee, Yoichi Ogo, and Hiroshi Yanagi for technical support. This work was financially supported by Ministry of Education, Culture, Sports, Science and Technology, Japan (Elements Science and Technology Project).

*Also at Japan Science and Technology Agency, Kawaguchi 332-0012, Japan; susaki@msl.titech.ac.jp

†Also at Frontier Research Center, Tokyo Institute of Technology, Nagatsuta, Midori, Yokohama 226-8503, Japan and Materials and Structures Laboratory, Tokyo Institute of Technology, Nagatsuta, Midori, Yokohama 226-8503, Japan.

¹S. M. Sze, *Physics of Semiconductor Devices*, 2nd ed. (Wiley, New York, 1981).

²J. Goniakowski and C. Noguera, *Interface Sci.* **12**, 93 (2004).

³G. Butti, M. I. Trioni, and H. Ishida, *Phys. Rev. B* **70**, 195425 (2004).

- ⁴L. Giordano, F. Cinquini, and G. Pacchioni, *Phys. Rev. B* **73**, 045414 (2006).
- ⁵S. Prada, U. Martinez, and G. Pacchioni, *Phys. Rev. B* **78**, 235423 (2008).
- ⁶S. Schintke, S. Messerli, M. Pivetta, F. Patthey, L. Libioulle, M. Stengel, A. De Vita, and W. D. Schneider, *Phys. Rev. Lett.* **87**, 276801 (2001).
- ⁷T. König, G. H. Simon, H.-P. Rust, and M. Heyde, *J. Phys. Chem. C* **113**, 11301 (2009).
- ⁸M. Bielezki, T. Hynninen, T. M. Soini, M. Pivetta, C. R. Henry, A. S. Foster, F. Esch, C. Barth, and U. Heiza, *PhysChemChemPhys* **12**, 3203 (2010).
- ⁹M. E. Vaida, T. Gleitsmann, R. Tshitnga, and T. M. Bernhardt, *J. Phys. Chem. C* **113**, 10264 (2009).
- ¹⁰S. Yuasa, T. Nagahama, A. Fukushima, Y. Suzuki, and K. Ando, *Nat. Mater.* **3**, 868 (2004).
- ¹¹D. E. Eastman, *Phys. Rev. B* **2**, 1 (1970).
- ¹²G. Chern, *Surf. Sci.* **387**, 183 (1997).
- ¹³Y. W. Chung and W. B. Weissbard, *Phys. Rev. B* **20**, 3456 (1979).
- ¹⁴M. Pfeiffer, K. Leo, and N. Karl, *J. Appl. Phys.* **80**, 6880 (1996).
- ¹⁵H. Ishii, N. Hayashi, E. Ito, Y. Washizu, K. Sugi, Y. Kimura, M. Niwano, Y. Ouchi, and K. Seki, *Phys. Status Solidi A* **201**, 1075 (2004).
- ¹⁶B. Henderson and D. H. Bowen, *J. Phys. C* **4**, 1487 (1971).
- ¹⁷P. Casek, F. Finocchi, and C. Noguera, *Phys. Rev. B* **72**, 205308 (2005).
- ¹⁸J. Y. Lim, J. S. Oh, B. D. Ko, J. W. Cho, S. O. Kang, G. Cho, H. S. Uhm, and E. H. Choi, *J. Appl. Phys.* **94**, 764 (2003).
- ¹⁹J. P. Boeuf, *J. Phys. D* **36**, R53 (2003).
- ²⁰D. J. Driscoll, W. Martin, J.-X. Wang, and J. H. Lunsford, *J. Am. Chem. Soc.* **107**, 58 (1985).
- ²¹T. Itoh and J. H. Lunsford, *Nature (London)* **314**, 721 (1985).
- ²²S. Altieri, L. H. Tjeng, and G. A. Sawatzky, *Phys. Rev. B* **61**, 16948 (2000).
- ²³K. Teramura, T. Tanaka, H. Ishikawa, Y. Kohno, and T. Funabiki, *J. Phys. Chem. B* **108**, 346 (2004).
- ²⁴H.-J. Freund and G. Pacchioni, *Chem. Soc. Rev.* **37**, 2224 (2008).
- ²⁵C. Harding, V. Habibpour, S. Kunz, A. N.-S. Farnbacher, U. Heiz, B. Yoon, and U. Landman, *J. Am. Chem. Soc.* **131**, 538 (2009).